Journal of The Electrochemical Society, **164** (4) E42-E47 (2017)
0013-4651/2017/164(4)/E42/6/$37.00 © The Electrochemical Society

Combination of Cumulative and Convergent Flows as a Means to Improve the Uniformity of Tertiary Current Distribution in Parallel-Plate Electrochemical Reactors

A. N. Colli[z] **and J. M. Bisang**

Universidad Nacional del Litoral, CONICET, Programa de Electroquímica Aplicada e Ingeniería Electroquímica (PRELINE), Facultad de Ingeniería Química, S3000AOM Santa Fe, Argentina

The study of current distribution is usually made in order to determine the performance of an electrochemical reactor. A comparison of the different types of current distributions is performed concluding that the tertiary one is the most unfavorable in parallel-plate electrochemical reactors. To overcome the problem, a reactor with a perpendicular and cumulative flow at the inlet region coupled with a convergent flow along the axial length, based on previous experimentally validated ideas,[1,2] is theoretically analyzed for laminar flow conditions. This configuration allows an important improvement in the reactor performance characterized by a more uniform current distribution under limiting current conditions.
© 2017 The Electrochemical Society. [DOI: 10.1149/2.0521704jes] All rights reserved.

Manuscript received January 12, 2017. Published January 31, 2017.

The parallel plate geometry, usually in a filter-press arrangement, provides a multipurpose device for many electrochemical applications. Parallel plate cells have many advantages:[3] (i) the geometry is willingly scaled by increasing the electrode area or incorporation into a multiple cell stacks, (ii) a wide range of electrode materials is available, (iii) the reaction environment is more or less well know, with regards of fluid flow, mass transport and residence time distributions, (iv) experiences of such cells in industrial practice are relatively well documented in the fields of electro-synthesis, electrochemical processing, environmental treatment and flow batteries for energy storage.

For economic reasons, it is generally advantageous to work at high reaction rates in order to achieve a greater production volume, requiring good mass-transfer conditions in the electrochemical reactor. Moreover, a uniform current distribution gets as advantages high quality of product and durability of the electrode.

A non-uniform current distribution brings unwanted effects by the appearance of side reactions and decreasing in the cell performance. Additionally, in the case of metal deposition can lead to the depletion of metal ions near the surface of the electrode in the regions of high current densities, which produces several problems such as: quality of deposits, change in their morphology, different thicknesses in the coating, dendritic growth with the possibility of short circuit and variation of alloy composition.[4] In organic electro-synthesis affects the selectivity of the products. In flow batteries influence the operating time in loading and unloading processes.[5] In fuel cells generates excessive losses of potencial, decreasing the efficiency and durability of the cell.[6] While in lithium ion batteries it causes uneven utilization of the active materials, decreasing the energy density and the degradation of the cell.[7] Thus, maintaining a uniform current distribution is an extremely important issue for practical applications of electrochemical systems.

Electrochemical reactors with parallel-plate electrodes have a non-uniform mass transfer distribution along the axial position due to: (i) a vast reaction rate at the entrance because of the low resistance to mass transfer in the region where the starting solution is brought into contact with the electrode; and (ii) a decrease in the reaction rate with the axial position as a result of the developing of the boundary layer along the electrode length. To overcome both problems the use of turbulence promoters has been proposed,[8] which becomes more uniform the velocity profile[9] inside the reactor and also increase the reaction rate and improve the current distribution.[10] However, turbulence promoters increase the pressure drop across the reactor and clog a part of the electrode surface area. Moreover, depending on the promoter type, preferential channels for the flow patterns can be generated reducing the efficiency of the equipment.[9]

Jorne[11] proposed a cumulative flow channel with the inlet of the solution through a porous electrode facing the active electrode. In this arrangement, the velocity increases linearly along the electrode length and hence the diffusion boundary layer becomes constant, showing uniform accessibility to mass-transfer. Recently, it has been evaluated the performance of tubular electrochemical reactors using computational fluid dynamics.[12,13] Additionally, a tubular reactor with axial and tangential entries has been modelled,[14] finding that in laminar flow tangential inlet equalizes the distribution of the local mass-transfer coefficients, although experimental results indicate otherwise. Prentice and Tobias[15] studied theoretically the influence of auxiliary electrodes and insulating plates on the secondary current distribution of a curved electrode. Mehdizadeh et al.[16] used a numerical model that takes into account the secondary current distribution, to increase the uniformity of current distribution in a planar electrode by using a coplanar auxiliary electrode. Lavelaine de Maubeuge[17] proposed a theoretical method to deduce the geometry of a reactor from the desired local current density assuming a fast kinetics without mass-transfer limitations. Other arrangements with uniform cell injection have been theoretically[18] and experimentally[19] studied, showing an almost uniform primary and tertiary current distributions but its construction is difficult in large-scale applications. To counteract the marked current distribution at the reactor inlet in parallel-plate electrochemical reactors, in a previous work[1] was analyzed a perpendicular and cumulative inlet flow. This improvement is most noticeable for short reactors, because in long reactors the decrease in the mass-transfer coefficient along the electrode length has a strong influence on the performance of the equipment. Likewise, the use of a convergent flow allowed to increase the current density at the reactor outlet.[2]

The aim of this paper is to analyze theoretically, based on our previous experimentally validated ideas,[1,2] a combination of cumulative flow and convergent flow in order to become more uniform the current distribution at parallel-plate electrochemical reactors under laminar flow conditions.

Current Distribution at Conventional Parallel-Plate Electrodes

The primary current distribution at an electrochemical reactor conformed by parallel-plate electrodes embedded in the walls of a flow channel, as it is sketched in Figure 1, is given by the following analytical expression[20]

$$\frac{j_x}{j_{av}} = \frac{\Omega \cosh(\Omega) / K\left[\tanh^2(\Omega)\right]}{\sqrt{\sinh^2(\Omega) - \sinh^2\left[\Omega\left(2x/L - 1\right)\right]}} \qquad [1]$$

where K is the complete elliptic integral of the first kind, that can be approximated by

$$K(x) = \ln(2) + x \qquad [2]$$

[z]E-mail: ancolli@gmail.com

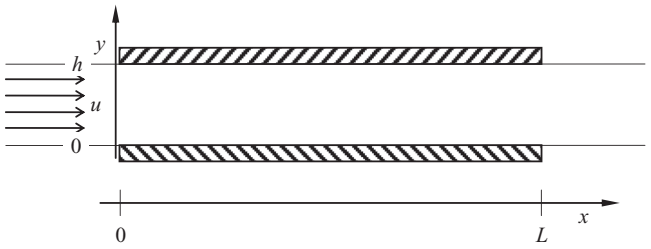

Figure 1. Schematic representation of parallel plate electrodes in a channel flow.

when $x > \pi$.[21] The average value of current density, j_{av}, is defined as

$$j_{av} = \frac{1}{A}\int_0^A j_x \mathrm{d}A \qquad [3]$$

Secondary current distribution occurs when there is a surface overpotential but without any influence of mass-transfer. Wagner[22] demonstrated that the secondary current distribution is always less marked than the primary one.

Tertiary current distributions take into account the mass-transfer effect on the reaction kinetics. For a parallel-plate electrochemical reactor with wide electrodes under laminar flow conditions, the local mass-transfer coefficient, $k_{m,x}$, is given by[23]

$$k_{m,x} = \frac{D\sqrt{\varepsilon}}{d_h \Gamma\left(4/3\right)}\left(\frac{\mathrm{ReSc}}{9\int_0^{x/d_h}\sqrt{\varepsilon}\,\mathrm{d}\left(x/d_h\right)}\right)^{1/3} \qquad [4]$$

being ε the dimensionless velocity profile at the electrode surface given by

$$\varepsilon = \left.\frac{\partial\left(u_x/u_{av}\right)}{\partial\left(y/d_h\right)}\right|_{(y/d_h)=0} \qquad [5]$$

Solving Eq. 4 with different theoretical velocity profiles, yields

$$k_{m,x} = a\mathrm{Sc}^{1/3}\frac{D}{d_h^{1-1/n}}\left(\frac{\mathrm{Re}}{x}\right)^{1/n} \qquad [6]$$

The local current density at the working electrode for a mass-transfer controlled reaction under limiting current conditions is given by

$$j_x = \nu_e F k_{m,x} c_b \qquad [7]$$

Introducing Eq. 6 into Eqs. 7 and 3 and solving, yields

$$\frac{j_x}{j_{av}} = \frac{n-1}{n}(x/L)^{-1/n} \qquad [8]$$

For a parallel-plate electrochemical reactor with infinitely wide electrodes and fully developed laminar flow, n is 3, and the current distribution results in[24]

$$\frac{j_x}{j_{av}} = \frac{2}{3}(x/L)^{-1/3} \qquad [9]$$

According to the boundary layer theory, for developing laminar flow is $n = 2$,[23,25,26] giving

$$\frac{j_x}{j_{av}} = \frac{1}{2}(x/L)^{-1/2} \qquad [10]$$

Colli and Bisang[23] concluded that the exponent in the Reynolds number in empirical laminar mass-transfer correlations must ranged from 1/2, according to the boundary layer theory, to 1/3, under fully developed flow conditions. Then, the limiting current distributions under laminar flow are necessarily between Eqs. 9 and 10. However, an improper design of the flow distributors can result in current distributions even more marked.

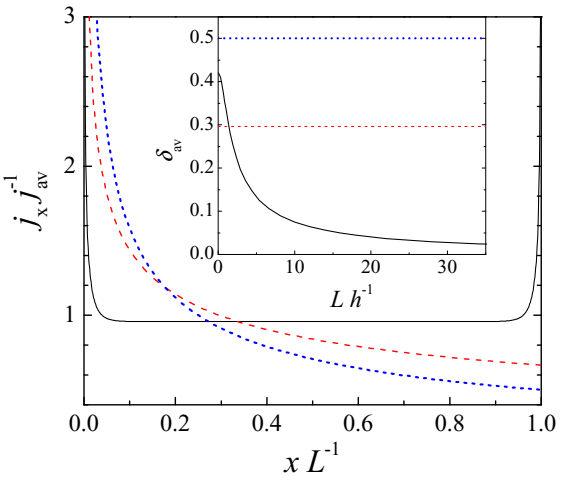

Figure 2. Current distributions in an electrochemical reactor with parallel-plate electrodes. Full black line: primary current distribution, Eq. 1, with $L\,h^{-1} = 5$. Dashed and dotted lines: tertiary current distribution. Dashed red line: Eq. 9. Dotted blue line: Eq. 10. Inset: mean relative deviation of the primary and tertiary current distributions as a function of the aspect ratio $L\,h^{-1}$.

Figure 2 shows a comparison between the current distributions above presented. The full black line represents the primary current distribution, Eq. 1, with an aspect ratio $L\,h^{-1} = 5$. The dashed red line shows the case of mass-transfer control under limiting current conditions for a reactor with infinitely wide electrodes and fully developed laminar flow, Eq. 9, and the dotted blue line according to the boundary layer theory, Eq. 10. From Figure 2 it is qualitatively inferred that the tertiary current distribution is more pronounced than the primary one.

To quantify the uniformity in the current distributions the mean relative deviation, δ_{av}, is defined as

$$\delta_{av} = \frac{1}{L}\int_0^L \left|\frac{j_x}{j_{av}} - 1\right|\mathrm{d}x \qquad [11]$$

Thus, the current distribution is more uniform as δ_{av} is smaller. Introducing Eq. 8 into Eq. 11 the mean relative deviations is given by

$$\delta_{av} = 2\frac{(n-1)^{n-1}}{n^n} \qquad [12]$$

resulting 8/27 or 1/2 for the case of Eq. 9 or Eq. 10, respectively. The inset in Figure 2 shows δ_{av} as a function of the aspect ratio $L\,h^{-1}$ for the primary, full black line, and tertiary current distributions, dashed red and dotted blue lines. The primary current distribution is more marked than the tertiary one only in a narrow range of aspect ratios from 0 to 1.5, which represents unrealistic reactors. Equipments used in the industrial practice present aspect ratios higher than 50 being negligible the primary current distribution, and the secondary distribution is even least marked. However, the main problem in parallel-plate electrodes is the tertiary current distribution, represented under laminar flow conditions by the region between the dashed red and dotted blue lines in Figure 2.[23]

Mathematical Modelling of the Tertiary Current Distribution

Figure 3, part (a), sketches the 3D modelled electrochemical system, consisting in the inlet region of a rectangular flow channel. Thus, at $y = h$ for $0 \le x \le l_e$ the electrolyte is uniformly fed through a port facing the working electrode. The port has the same width as the electrode and the end of the channel is closed off. Here, the flow is cumulative and the average velocity flow increases linearly along the length of the port and the working electrode is uniformly accessible to mass-transfer in the inlet region of the reactor. The working electrode lengthens for $l_e \le x \le L$ where the reactor presents a continuous reduction of the cross-section area for the solution flow, impeding a

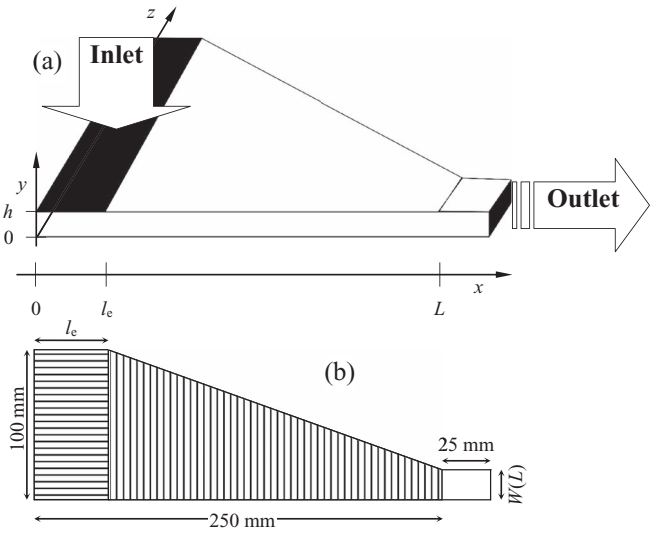

Figure 3. (a) Schematic view of the reactor. (b) Dimensions of the computational domain for the modelling of an electrochemical reactor with perpendicular cumulative inlet flow, horizontal dashed region, associated to convergent flow, vertical dashed region. $l_e = 50$ or 75 mm. $W(L) = 20$ mm ($\lambda = 0.8$), 15 mm ($\lambda = 0.85$) or 10 mm ($\lambda = 0.9$).

developed flow as a means of improving mass-transfer at the electrode length. Thus, the flow becomes convergent. The convergence ratio, λ, is defined as[2]

$$\lambda = 1 - \frac{W(L)}{W(l_e)} \qquad [13]$$

In this region, the working electrode faces the counter electrode that covers the opposite wall of the channel flow. It must be remarked that the primary current distribution caused by the necessary displacement of the counter electrode to enable the perpendicular inlet flow of electrolyte is completely counteracted by the tertiary current distribution.[1]

The local current density at the working electrode is also given by

$$j_x = \nu_e F D \left.\frac{dc(x,y)}{dy}\right|_{y=0} \qquad [14]$$

The calculation of the concentration gradient at the surface of the working electrode requires to solve the convective mass-transfer equation, according to

$$u_x\frac{\partial c}{\partial x} + u_y\frac{\partial c}{\partial y} + u_z\frac{\partial c}{\partial z} = D\left(\frac{\partial^2 c}{\partial x^2} + \frac{\partial^2 c}{\partial y^2} + \frac{\partial^2 c}{\partial z^2}\right) \qquad [15]$$

which were obtained from the simultaneous solution of Navier-Stokes equations with the continuity equation. The OpenFOAM free software was used to calculate the velocity and concentration fields. The velocity profiles inside the reactor were calculated with the iterative use of the simpleFOAM routine[27,28] in steady state laminar flow. Thus, the Navier-Stokes equations coupled to the continuity equation were numerically solved. The field of concentration was obtained with the use of the scalarTransportFoam routine by using the velocity profiles previously obtained. It was assumed that the concentration and velocity profiles are uniform at the reactor inlet in the x direction, with $u_y = u_z = 0$, whereas the pressure is uniform. Likewise, it was considered that the concentration and velocity gradients are zero at the reactor outlet,[27] while the pressure is zero. A non-slip boundary condition was used at the solid walls. The concentration was set to zero at the working electrode and the concentration gradients were null for the other solid walls. The absolute tolerances for calculating the velocity, pressure and concentration profiles were 1×10^{-5}, 1×10^{-6} y 1×10^{-6}, respectively. The relaxation factor was 0.3 for pressure and 0.7 for velocity. The computational region was divided into a structured mesh

Table I. Physicochemical properties, geometrical and hydrodynamic parameters used in the simulation.

Kinematic viscosity = ν, m^2/s	1.31×10^{-6}
Diffusion coefficient = D, m^2/s	8.10×10^{-10}
Volumetric flow rate, dm^3/h	5.85–90
Reynolds number = Re*	24.8–380
Hydraulic diameter = d_h, mm	10
Electrode length = L, mm	250
Length of cumulative inlet region = l_e, mm	50, 75
Inlet electrode width = W(x = 0), mm	100
Outlet electrode width = W(x = L), mm	10, 15, 20
Convergence ratio = λ	0.9, 0.85, 0.8

*calculated with the mean velocity at the inlet of the convergent region.

180 per 85 per 70 cells in x-y-z directions, respectively. A non-uniform mesh grading was used for the mesh size in the y direction, Δy, which was gradually varied according to a geometric progression with a ratio of 5 between the size of the farthest cell and the nearest one to the working electrode. A similar numerical calculation procedure was successfully used[2] to predict experimental results in an electrochemical reactor only with convergent flow. The geometric dimensions of the computational domain are given in Figure 3, part (b) and Table I. The physicochemical properties and hydrodynamic parameters used in the calculations, based in our previous experimental papers[1,2,23] using the electrochemical reduction of ferricyanide from solutions with $[K_3Fe(CN)_6]$-$[K_4Fe(CN)_6]$ 0.01 mol dm^{-3} as test reaction, in 0.65 mol dm^{-3} of K_2CO_3 as supporting electrolyte at 30°C, are also summarized in Table I. This procedure was employed to calculate the current distributions instead of the use of Eq. 4 because this equation is valid for reactors with a high ratio between the electrode width and the interelectrode gap. This assumption is not fulfilled for the proposed geometry in the last part of the convergent region.

Results and Discussion

Figure 4 shows typical curves of the slope in the velocity profile at the electrode surface along the entire electrode length according to the numerical solution of the Navier-Stokes equations. The Reynolds number was calculated using the average velocity at the inlet of the convergent region and ε was evaluated with the average velocity at each axial position in the reactor. It is observed a linear increase of ε, in the region of the perpendicular flow inlet. The dimensionless profile velocity approaches the value of 12, characteristic of developed

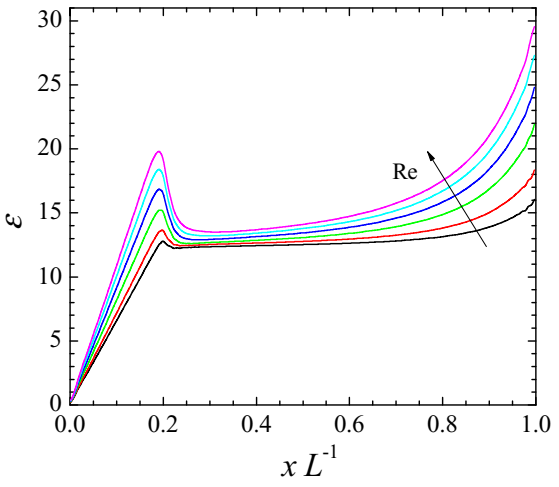

Figure 4. Slope of the velocity profile at the electrode surface as a function of the dimensionless axial position along the reactor according to the numerical solutions of the Navier-Stokes equations. Re = 24.8, 49.6, 100, 150, 200, and 250. $\lambda = 0.85$. $l_e = 50$ mm.

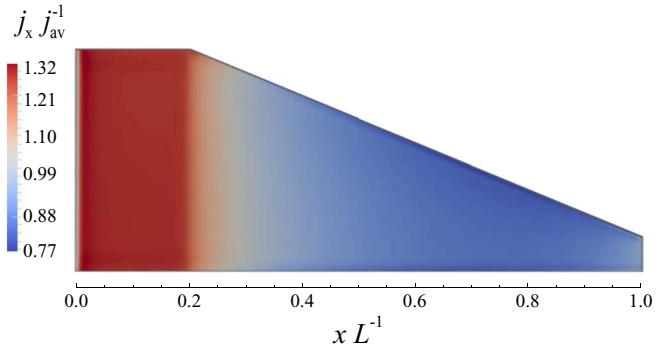

Figure 5. Contour plot of the limiting current distribution as a function of the position for an electrochemical reactor with perpendicular cumulative inlet flow associated to convergent flow. Re = 49.6. λ = 0.85. l_e = 50 mm.

flow,[29] at the beginning of the convergent region and a pronounced growth of ε takes place at the end of the electrode due to the effect of the convergent flow on the hydrodynamics. This behavior is an improvement with regards to the usually constant ε value shown in conventional parallel plate reactors when the flow is developed.

Figure 5 presents a typical contour plot of the limiting current distribution along the electrode length at a Reynolds number of 49.6, λ = 0.85 and l_e = 50 mm, for an electrochemical reactor with a combined arrangement of perpendicular cumulative inlet flow associated to convergent flow. It can be seen that the maximum value of the current distribution is achieved in the entrance zone given by 1.32 times the average value with a minimum of 0.77 for *x*/*L* ranging from 0.7 to 0.85.

Figure 6 compares the limiting current distributions for an electrochemical reactor with perpendicular cumulative inlet flow associated to convergent flow for λ = 0.85 and l_e = 50 mm, represented as thick full lines for different Reynolds numbers, with those for a conventional parallel-plate arrangement according to Eq. 9, dashed line, and Eq. 10, dotted line. Figure 6 also reports that a small enhancement in the uniformity of the distribution of reaction rates can be achieved decreasing the fluid velocity at the reactor entrance. The inset in Figure 6 contrasts δ_{av} as a function of the Reynolds number for the proposed reactor, (■), with those of the tertiary current distributions according to Eqs. 9 and 10. A significant improvement in the reactor performance can be observed, giving a mean relative deviation in the range from 0.19 to 0.245. Furthermore, the symbols (●) correspond to a reactor with a conventional inlet flow and infinitely wide parallel-plate electrodes under developing laminar flow according to the Sparrow et al.[30] model for the velocity profile, being 10 mm the hydraulic diameter. These points were obtained using the analytical procedure reported previously,[23] which give identical results to the numerical calculation above reported. Thus, the comparison between the dashed line with the symbols (●) shows the effect of the developing laminar flow on the uniformity of the current distribution, showing a similar behavior for lower Re numbers and a slightly less uniform distribution when the Reynolds number is increased.

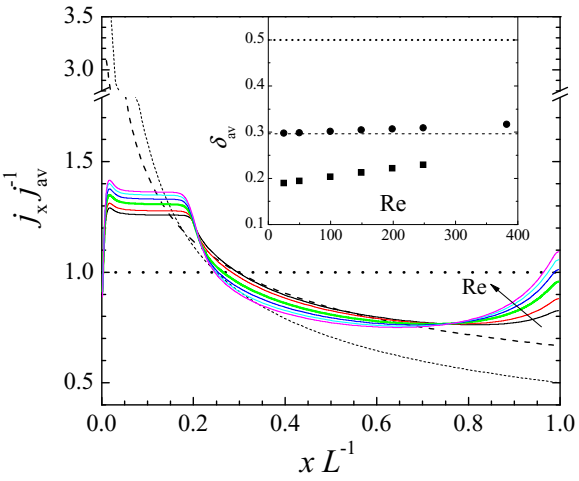

Figure 6. Comparison of the limiting current distribution for an electrochemical reactor with perpendicular cumulative inlet flow associated to convergent flow at different Reynolds numbers, thick full lines, with those for a conventional arrangement of parallel-plate electrodes given by Eq. 9, dashed line, and Eq. 10, dotted line. Re = 24.8, 49.6, 100, 150, 200, and 250. λ = 0.85. l_e = 50 mm. Inset: mean relative deviation of the tertiary current distributions as a function of the Reynolds number. (■): proposed reactor. Dashed line: Eq. 9. Dotted line: Eq. 10. (●): reactor with a conventional inlet and infinitely wide parallel-plate electrodes under developing laminar flow.[23]

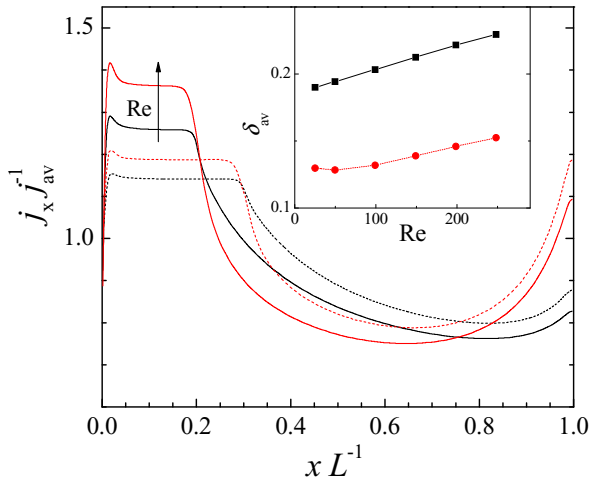

Figure 7. Effect of the length of the cumulative region on the current distribution as a function of the Reynolds number. Re = 24.8 and 250. λ = 0.85. Inset: mean relative deviation of the tertiary current distributions as a function of the Reynolds number. Full lines: l_e = 50 mm. Dashed lines: l_e = 75 mm.

Figure 7 displays the effect of the length of the cumulative region on the current distribution at different Reynolds numbers for λ = 0.85. The inset in Figure 7 reveals that an important improvement in the uniformity can be obtained by increasing the ratio between the area for the inlet flow and the total area of the electrode.

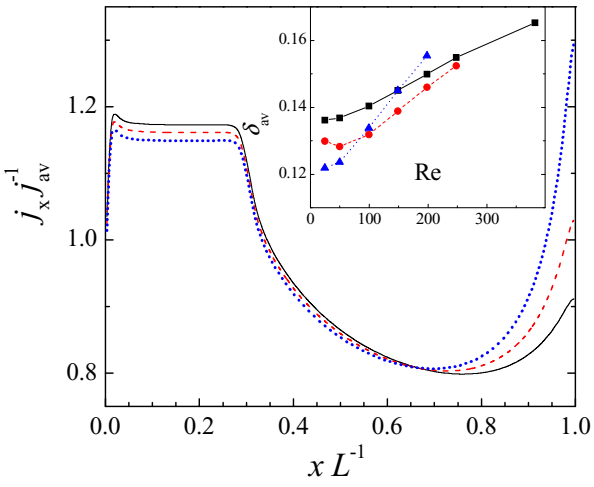

Figure 8. Effect of the convergence ratio on the current distribution. Re = 100. l_e = 75 mm. Inset: mean relative deviation of the tertiary current distributions as a function of the Reynolds number. Full line: λ = 0.8. Dashed line: λ = 0.85. Dotted line: λ = 0.9.

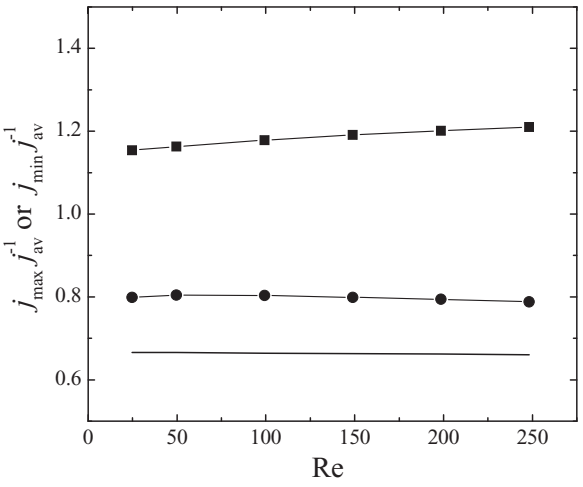

Figure 9. Maximum (■) and minimum (●) current densities, related to the average value, as a function of the Reynolds number for the electrochemical reactor with perpendicular cumulative inlet flow associated to convergent flow. $\lambda = 0.85$. $l_e = 75$ mm. Full line: minimum current density corresponding to a reactor with a conventional inlet and infinitely wide parallel-plate electrodes under developing laminar flow.[23]

Figure 8 shows the influence of the convergence ratio on the current distribution at a Reynolds number of 100 for $l_e = 75$ mm. The range of the Reynolds number reported in the inset was diminished in order to ensure laminar flow conditions at the reactor outlet. For the larger value of λ, it is observed a pronounced increase in the current distribution in the convergent region, which represents an unacceptable behavior. However, the inset reveals that the mean relative deviation diminishes when the Reynolds number is lower achieving minimal values, ranging from 0.13 to 0.15, for $\lambda = 0.85$ in a wide range of Reynolds numbers. These mean relative deviations are similar than those obtained under turbulent flow conditions.[2]

Figure 9 reports on the maximum and minimum current densities, related to the average value, as a function of the Reynolds number for the electrochemical reactor with perpendicular cumulative inlet flow associated to convergent flow for $\lambda = 0.85$ and $l_e = 75$ mm. The maximum ratio is 1.18 and the minimal one is 0.80. Taking into account Eq. 9 these values are achieved in a conventional reactor at xL^{-1} 0.18 and 0.58, respectively. It is also showed, as full line, the minimum current density corresponding to a reactor with a conventional inlet and infinitely wide parallel-plate electrodes under developing laminar flow.[23] It is important to note that the maximum current density for the latter case is not shown due to its high value. Thus, the proposed geometry of parallel-plate electrodes homogenizes the current distribution in a large fraction of the electrode, by increasing the current density at the end of the reactor and simultaneously the high values at the inlet are restricted. Both actions improve the reactor performance.

Conclusions

1. The tertiary current distribution is frequently more pronounced than the primary and secondary ones in industrial electrochemical reactors, conditioning the design of these equipments.
2. For a given value of the Reynolds number, at each length of the cumulative region, there is an optimum in the convergent ratio in order to obtain a minimum mean relative deviation. Likewise, in all cases the current distribution is more uniform when the Reynolds number decreases.
3. The use of a combined arrangement formed by a perpendicular and cumulative inlet flow zone coupled with a final convergent flow region allows homogenising the tertiary current distribution in parallel-plate electrochemical reactors, which represents a promising alternative to improve the performance of the reactors under laminar flow conditions.

Acknowledgments

This work was supported by the Agencia Nacional de Promoción Científica y Tecnológica (ANPCyT), Consejo Nacional de Investigaciones Científicas y Técnicas (CONICET) and Universidad Nacional del Litoral (UNL) of Argentina.

List of Symbols

a	constant depending on the hydrodynamics
A	electrode surface area, m^2
c	concentration, mol/m^3
D	diffusion coefficient, m^2/s
d_h	hydraulic diameter $= 2h$, m
F	Faraday constant, 96485 C/mol
h	interelectrode gap, m
j	current density, A/m^2
K	complete elliptic integral of the first kind approximated by Eq. 2
k_m	mass-transfer coefficient, m/s
L	electrode length, m
l_e	cumulative entrance length, m
n	constant depending on the hydrodynamics
Re	Reynolds number $= u_{av}d_h/\nu$
Sc	Schmidt number $= \nu/D$
u	fluid velocity, m/s
W	electrode width, m
x	axial coordinate, m
y	axial coordinate, m
z	axial coordinate, m

Greek

Γ(4/3)	4/3 Gamma function ≈ 0.89
δ_{av}	mean relative deviation given by Eq. 11
ε	dimensionless velocity profile at the electrode surface given by Eq. 5
λ	convergence ratio defined by Eq. 13
ν	kinematic viscosity, m^2/s
ν_e	charge number of the electrode reaction
Ω	dimensionless variable $= \pi L/(2h)$

Subscripts

av	average value
b	bulk
max	maximum value
min	minimum value
x	the variable is referred to the x coordinate
y	the variable is referred to the y coordinate
z	the variable is referred to the z coordinate

References

1. A. N. Colli and J. M. Bisang, *Electrochim. Acta*, **137**, 758 (2014).
2. A. N. Colli and J. M. Bisang, *Electrochim. Acta*, **113**, 575 (2013).
3. F. C. Walsh and D. Pletcher, in *Developments in Electrochemistry: Science Inspired by Martin Fleischmann*, D. Pletcher, Z.-Q. Tian, and D. Williams Editors, p. 95, John Wiley & Sons, Ltd., (2014).
4. R. C. Alkire, *J. Chem. Educ.*, **60**, 274 (1983).
5. R. G. A. Wills, J. Collins, D. Stratton-Campbell, C. T. J. Low, D. Pletcher, and F. Walsh, *J. Appl. Electrochem.*, **40**, 955 (2010).
6. M. Eisenberg, in *Advances in Electrochemistry and Electrochemical Engineering, Vol. 2 - Electrochemical Engineering*, C. W. Tobias Editor, p. 235, Interscience Publishers, New York, (1962).
7. G. Zhang, C. E. Shaffer, C.-Y. Wang, and C. D. Rahn, *J. Electrochem. Soc.*, **160**, A2299 (2013).
8. W. M. Taama, R. E. Plimley, and K. Scott, *Electrochim. Acta*, **41**, 543 (1996).
9. A. N. Colli and J. M. Bisang, *Electrochim. Acta*, **56**, 7312 (2011).
10. A. N. Colli, R. Toelzer, M. E. H. Bergmann, and J. M. Bisang, *Electrochim. Acta*, **100**, 78 (2013).
11. J. Jorne, *J. Electrochem. Soc.*, **129**, 1727 (1982).
12. S. A. Martínez-Delgadillo, H. R. Mollinedo, P. M. A. Gutiérrez, I. D. Barceló, and J. M. Méndez, *Comput. Chem. Eng.*, **34**, 491 (2010).

13. J. Wang, T. Li, M. Zhou, X. Li, and J. Yu, *Electrochim. Acta*, **173**, 698 (2015).
14. J. Esteban Duran, F. Taghipour, and M. Mohseni, *Int. J. Heat Mass Transfer*, **52**, 5390 (2009).
15. G. A. Prentice and C. W. Tobias, *J. Electrochem. Soc.*, **129**, 78 (1982).
16. S. Mehdizadeh, J. Dukovic, P. C. Andricacos, L. T. Romankiw, and H. Y. Cheh, *J. Electrochem. Soc.*, **137**, 110 (1990).
17. H. Lavelaine de Maubeuge, *J. Electrochem. Soc.*, **149**, C413 (2002).
18. J. A. Medina and D. T. Schwartz, *J. Electrochem. Soc.*, **142**, 451 (1995).
19. J. A. Medina, D. L. Sexton, and D. T. Schwartz, *J. Electrochem. Soc.*, **142**, 457 (1995).
20. W. R. Parrish and J. Newman, *J. Electrochem. Soc.*, **117**, 43 (1970).
21. F. Goodridge and K. Scott, *Electrochemical process engineering: a guide to the design of electrolytic plant*, Plenum Press (1995).
22. C. Wagner, *J. Electrochem. Soc.*, **98**, 116 (1951).
23. A. N. Colli and J. M. Bisang, *J. Electrochem. Soc.*, **160**, E5 (2013).
24. W. R. Parrish and J. Newman, *J. Electrochem. Soc.*, **116**, 169 (1969).
25. E. R. G. Eckert and R. M. Drake, *Heat and mass transfer, 2nd edition*, p. 530, McGraw-Hill, New york, (1985).
26. V. Levich, *Physicochemical Hydrodynamics*, p. 700, Prentice Hall, New Jersey, (1962).
27. H. H. K. Versteeg and W. Malalasekera, *An Introduction to Computational Fluid Dynamics: The Finite Volume Method*, Pearson Education Limited, (2007).
28. J. H. Ferziger and M. Perić, *Computational Methods for Fluid Dynamics*, Springer London, Limited, (2002).
29. F. White, *Viscous Fluid Flow*, p. 640, Mc Graw-Hill, Boston, (2005).
30. E. M. Sparrow, S. H. Lin, and T. S. Lundgren, *Physics of Fluids*, **7**, 338 (1964).